Micromagnetic and Mössbauer Spectroscopic Investigation of Strain-Induced Martensite in Austenitic Stainless Steel

I. Mészáros, M. Káldor, B. Hidasi, A. Vértes, and I. Czakó-Nagy

Strain-induced martensite in 18/8 austenitic stainless steel was studied. Magnetic measurements and Mössbauer spectroscopic investigations were performed to characterize the amount of α′-martensite due to room-temperature plastic tensile loading. The effects of cold work and annealing heat treatment were explored using magnetic Barkhausen noise, saturation polarization, coercive force, hardness, and conversion electron Mössbauer spectra measurements. The results of the magnetic measurements were compared to results obtained by Mössbauer spectroscopy. The suggested Barkhausen noise measurement technique proved to be a useful quantitative and nondestructive method for determining the ferromagnetic phase ratio of the studied alloy.

Keywords
austenitic stainless steel, martensite formation, mechanical working, strain hardening

1. Introduction

MARTENSITE may form in austenitic stainless steels during cooling below room temperature (thermally) or in response to cold work (mechanically). Two types of martensite can form spontaneously upon cooling or cold working: ε-martensite, which forms on close-packed (111) planes in the austenite and has a hexagonal close-packed (hcp) crystal structure; and body-centered cubic (bcc) α′-martensite, which forms as plates with (225) habit planes in groups bounded by faulted sheets of austenite on (111) planes (Ref 1, 2).

Deformation-induced or strain-induced martensite formation is a unique feature of austenitic stainless steels. The extent of strain-induced transformation of austenite to martensite depends on temperature, strain rate, and composition. Composition determines the stability of austenite. In particular, nickel increases the stacking fault energy and thus increases the austenite stability. Carbon has a similar effect; it is an extremely powerful gamma stabilizer. Consequently, higher-nickel-grade stainless steels develop less martensite than lower-nickel grades when cold worked to equivalent degrees. The low-carbon and the titanium- or niobium-stabilized grades are especially sensitive to strain-induced martensite formation (Ref 3).

Thermal martensite can form under the specific M_s temperature, and plastic deformation-induced martensite occurs under the M_d temperature, where M_d is usually higher than M_s. The M_s temperature decreases with increasing nickel content in 18% Cr steels.

I. Mészáros, M. Káldor, and **B. Hidasi,** Technical University of Budapest, Department of Electrical Engineering Materials, H-1111 Goldman sq. 3, Budapest, Hungary; **A. Vértes** and **I. Czakó-Nagy,** Eötvös Loránd University, Department of Nuclear Chemistry, H-1117 Pázmány Péter sétány 2, Budapest, Hungary.

The mechanical behavior of austenitic stainless steels during cold work can be described as follows (Ref 4):

- When austenite is stable and the stacking fault energy is high, glide of perfect dislocations is the principal mechanism of plastic deformation.
- When the stability of the austenite and the stacking fault energy decrease, four new modes of deformation become competitive with the glide of perfect dislocations:

1. Glide of partial dislocations
2. Microtwinning
3. $\gamma \rightarrow \varepsilon$ transformation
4. $\gamma \rightarrow \alpha'$ transformation directly or via the path $\gamma \rightarrow \varepsilon \rightarrow \alpha'$

The gradual transformation of austenite to strain-induced martensite increases the work hardening of these steels. The fine α′-martensite grains appear inside the austenite grains mainly at the intersections of shear bands, making the movement of dislocations more difficult. However, the α′-martensite is not an effective strengthener compared to the classical thermal martensite in iron-carbon systems.

The α′-phase is thermodynamically much more stable than the ε-phase. The ε-phase forms before the α′-phase during cold working of a low-carbon 18/8-type steel. At higher deformations, the amount of the previously formed ε-phase decreases with increasing deformation because the α′-martensite grows at the expense of the ε-phase (Ref 5). The transformations of austenite to ε- and α′-phases are diffusionless or military type.

The reverse transformation of ε-phase occur between 150 and 400 °C, followed by the reversion of α′-phase above 400 °C (Ref 3). Both the ε- and the α′-martensite transform directly into austenite phase.

All austenitic stainless steels are paramagnetic in the annealed, fully austenitic condition. The hcp ε-martensite is paramagnetic in contrast to the bcc α′-martensite, which is strongly ferromagnetic (hard magnetic) and the only magnetic phase in the low-carbon austenitic stainless steels (Ref 6). Therefore, the cold-worked austenitic

stainless steels have detectable magnetic properties that can be eliminated by annealing.

2. Experimental Method

The appearance of α′-martensite was investigated during cold work, and the disappearance of this phase was studied during the annealing process.

2.1 *Material*

The chemical composition of the 18/8-type titanium-stabilized austenitic stainless steel used in this investigation was Fe-0.08C-1.8Mn-0.98Si-17.8Cr-8.22Ni-0.32Mo-0.75Ti-0.036P-0.0275 (mass percent). Strip-shaped specimens, 25 mm wide and 180 mm long, were cut from the original 2 mm thick stainless steel plate. The specimens were annealed at 1100 °C for 1 h before water quenching to prevent carbide precipitation. The measured primary grain size of the annealed stainless steel specimens was 28 μm.

2.2 *Applied Measuring Methods*

The Barkhausen noise was investigated by using a sinusoidal (10 Hz) exciting magnetic field produced by a function generator and a power amplifier. The applied measuring head contained a U-shape magnetizing coil and a pickup coil perpendicular to the surface of the specimen. The signal of the pickup coil was processed by a 0.3 to 38 kHz bandpass filter and amplified with a gain of 100. A KRENZ TRB 4000 (Krenz Electronics, Inc., Chicago, IL) computer-controlled signal-analyzing device was used to process the noise. The applied sampling frequency was 100 kHz. The power spectrum was calculated from the digitized time signal and integrated between the frequency limits of 2 and 38 kHz. The obtained value, which is proportional to the energy of the Barkhausen noise (BN energy) in the investigated frequency range, was used to characterize the microstructural changes. The applied magnetizing field strength corresponds to the irreversible domain wall displacement range on the hysteresis loop. Details of the Barkhausen noise measuring apparatus and the applied measurement method have been described previously (Ref 7, 8).

The saturation polarization (J_{max}) was measured by a ballistic method. The largest applied external magnetic field strength was 8750 A/cm, which was sufficient for reaching the magnetic saturation of the ferromagnetic α′-phase:

$$J_{max} = B_s - \mu_0 H$$

where B_s is the saturation induction, H is the applied external magnetic field, and μ_0 is the magnetic permeability of the vacuum. In both series of experiments, the Vickers hardness was measured with a load of 98.1 N.

Mössbauer spectroscopy is an accurate and reliable measuring technique for determining the ferromagnetic/paramagnetic ratio of alloys (Ref 9). The conversion electron Mössbauer spectra (CEMS) were recorded by a Ranger (Texas Instruments, Inc., Attleboro, MA) conversion electron detector at room temperature using a spectrometer working with constant acceleration. The SIRIUS (Sirius Systems Technology, Pasadena, TX) program was used for fitting the spectra.

3. Results and Discussion

3.1 *First Experimental Series*

The as-annealed stainless steel specimens were elongated at room temperature (20 °C) up to about 50% strain and were subjected to a heat treatment at 520 °C for 30 min. The BN energy and the hardness values were measured. In this and in the second series of experiments, a very low elongation rate (1 mm/min) and continuous water cooling were used to ensure a specimen temperature of 20 °C during plastic tensile loading.

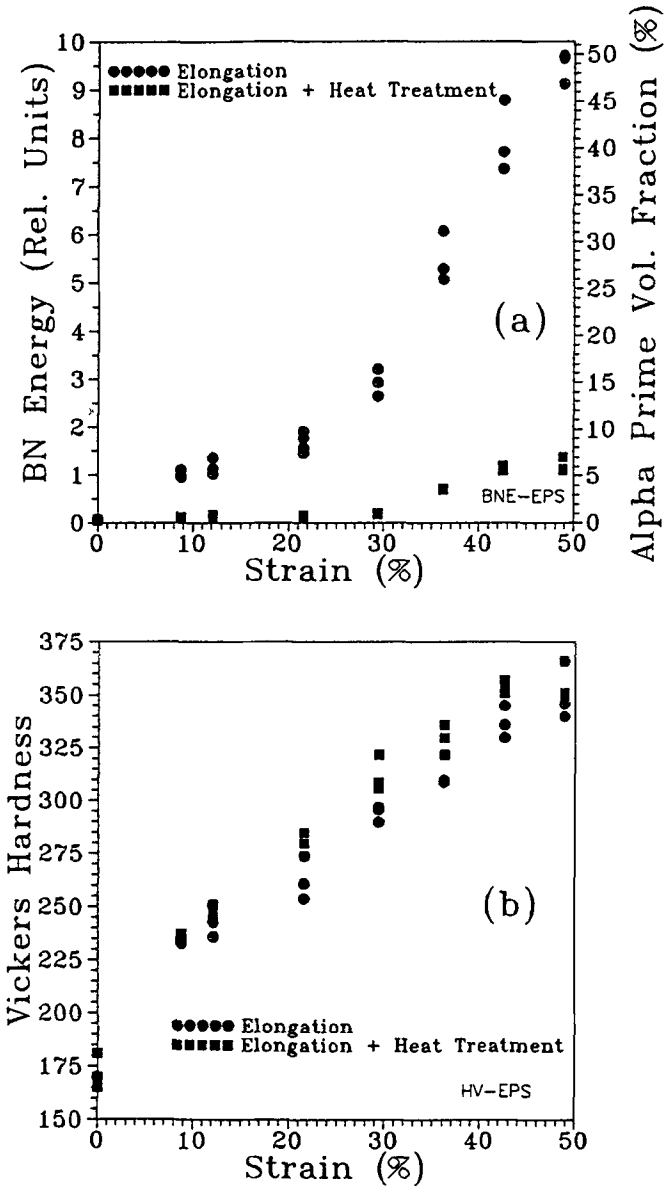

Fig. 1 Variation in BN energy (a) and hardness (b) as a function of strain

Figure 1(a) shows the variation of BN energy with strain during tensile deformation. It was observed that the BN energy increased with increasing elongation. The hardness also increased, nearly linearly, with increasing deformation in the 0 to 50% strain range (Fig. 1b). This result is in very good agreement with that obtained by Shrinivas et al. (Ref 10) for rolled type 304 austenitic stainless steel.

The heat treatment that followed the tensile deformation had a completely different effect on BN energy and hardness. The BN energy decreased rapidly, approaching the value that belongs to the undeformed state, whereas the hardness slightly increased.

3.2 *Second Experimental Series*

After annealing, the specimens were uniformly elongated at room temperature (20 °C) to a strain of $\varepsilon = 40\%$ and isochronally heat treated in the temperature range of 100 to 1000 °C for 30 min. The BN energy, magnetic saturation polarization, hardness, and CEMS were measured.

Figure 2 shows the variation in BN energy and hardness values as a function of isochronal heat treatment temperature. The BN energy started to decrease at about 350 to 400 °C and reached the zero level at 600 °C. The decrease in hardness values began at 600 °C, when the ferromagnetic phase (i.e., the α′-martensite) had already completely disappeared. The hardness approached the annealed level at 1000 °C. It must be noted that in the temperature range of 350 to 600 °C, where the α′-phase disappeared, the hardness increased in a small degree compared to its original level. To summarize, the magnetic and hardness recovery processes started at significantly different temperatures.

This behavior can be explained by the precipitation of carbides. If the annealed 18/8 steel is held in the 500 to 900 °C temperature range, the excess carbon precipitates in the form of chromium-rich face-centered cubic (fcc) $M_{23}C_6$ carbides. The carbides precipitate initially at grain boundaries, followed by precipitation at twin boundaries and finally at the austenite grain interior (Ref 3). The precipitation is rapid in the temperature range from 600 to 900 °C, and the cold work increases the rate of carbide formation, particularly in the grain interiors on dislocations. It is believed that in our experiment the carbide formation occurred simultaneously with the disappearance of α′-martensite in the 350 to 600 °C temperature range. The newly formed carbides could make the movement of dislocations difficult (similar to the α′-phase earlier).

The chromium-rich $M_{23}C_6$ carbides are stable below a temperature of about 1050 °C. Therefore, the reason that hardness decreases above 600 °C should be the decrease in the number of dislocations. However, the increase in carbide particles, which causes the distance between dislocations to increase, may have a similar effect on hardness according to the Orowan hardening mechanism.

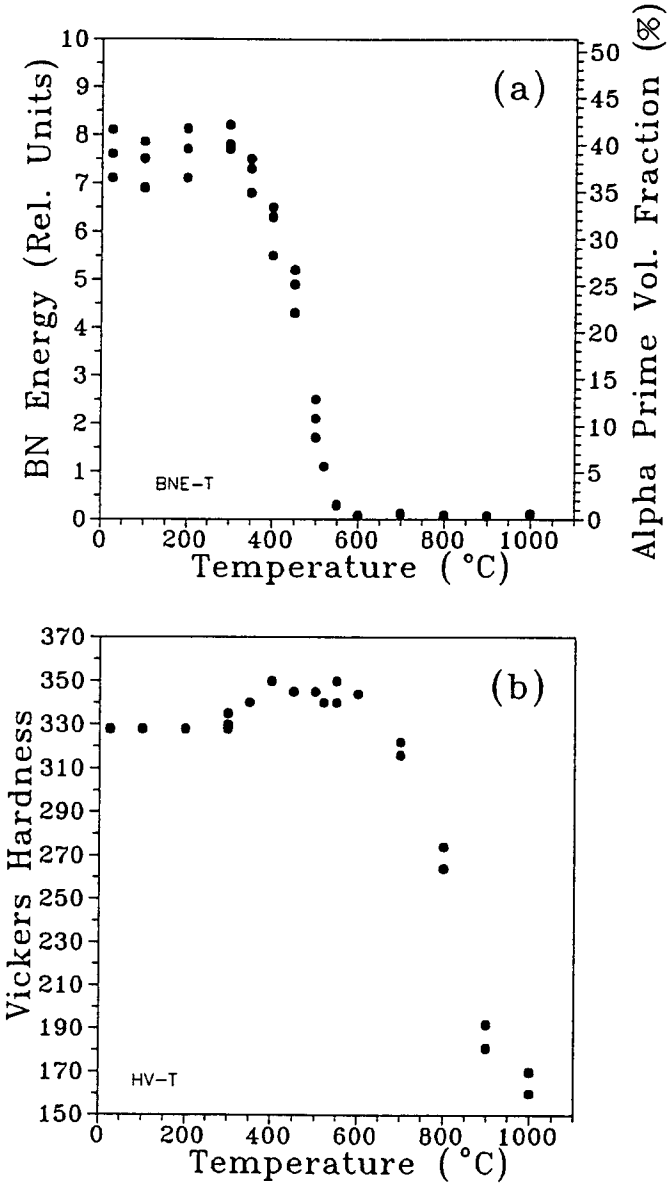

Fig. 2 Variation in BN energy (a) and hardness (b) as a function of temperature

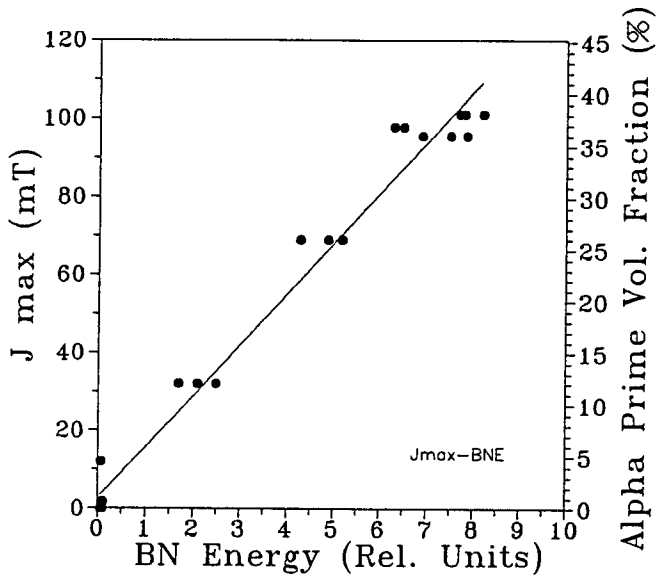

Fig. 3 Correlation between saturation polarization and BN energy

Good correlation was found between the measured BN energy and saturation polarization values (Fig. 3). The magnetic saturation polarization values are known to be proportional to the amount of ferromagnetic phase in the alloy. Consequently, we can state that the BN energy value is linearly proportional to the amount of the ferromagnetic phase, at least for the α′-martensite in the austenitic-type steels used in this study.

Four cold-worked stainless steel specimens were measured by conversion electron Mössbauer spectroscopy to determine quantitatively their ferromagnetic volume fraction. The room-temperature CEMS of two specimens from the second series of experiments are shown in Fig. 4. The isomer shift values refer to α-iron. It was assumed that the Debye-Waller factors are the same in both paramagnetic and ferromagnetic phases. The specimen that was heat treated at 100 °C contained 36% ferromagnetic α′-martensite according to the Mössbauer measurement. This point was used as a basis for calibrating the α′-phase volume fraction scales on the second vertical axes of Fig.1(a), 2(a), 3, and 5. As can be seen in Fig. 5, the results obtained by Mössbauer spectroscopy on the remaining three specimens are in very good agreement with our saturation polarization and BN energy results. This verifies the possibility of using BN energy measurement as a quantitative and nondestructive evaluation method for determining the ferromagnetic phase ratio in alloys.

According to Fig. 2(a), the reverse transformation of α′-phase back to austenite occurs between 350 and 600 °C. The hardness recovery process happens in temperature range of 600 to 1000 °C (Fig. 2b). The activation energy of the $\alpha' \rightarrow \gamma$ transformation and the virtual activation energy of the hardness recovery process were calculated from the results plotted in Fig. 2. According to the Arrhenius-type plot (Fig. 6) that was used, the slopes of the fitted linear functions are proportional to the activation energies of the thermal activated processes. The obtained activation energy for $\alpha' \rightarrow \gamma$ transformation is 57.4 kJ/mol. This value is about one-fifth of the activation energy of the iron atom self-diffusion in austenitic steels (Ref 11). The virtual activation energy of the hardness recovery process is 103 kJ/mol. The obtained activation energies are different, indicating that the processes that cause the hardness recovery are different from the $\alpha' \rightarrow \gamma$ transformation.

The magnetic properties of the strain-induced α′-martensite phase have been determined. The coercive force of α′-phase was measured by a ballistic method. The coercive force increased from 406 to 492 A/m in the 400 to 650 °C temperature range. It is believed that this was due to carbide precipitation

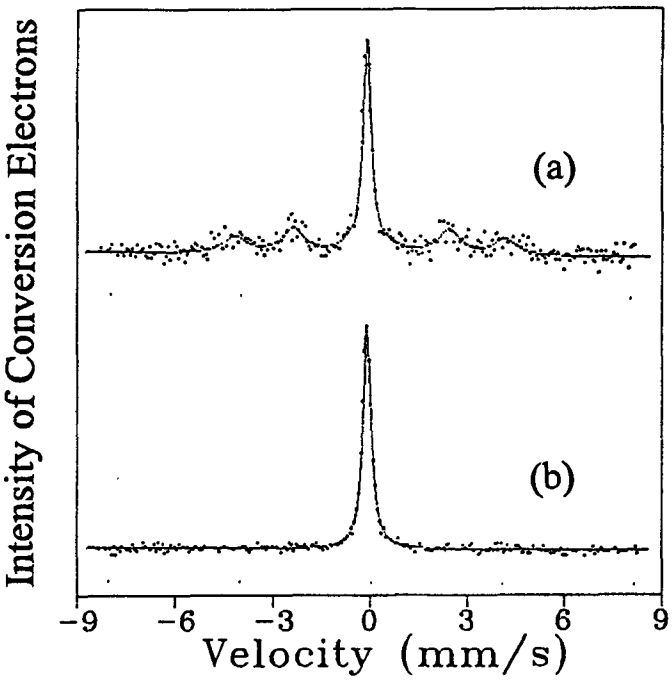

Fig. 4 Room temperature CEMS of specimens heat treated at 100 °C (a) and at 1000 °C (b)

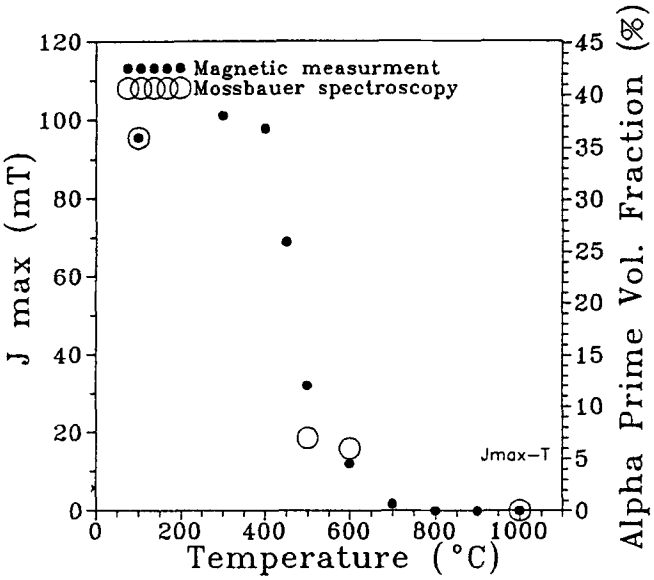

Fig. 5 Variation in magnetic saturation polarization and α′-phase volume fraction values obtained by Mössbauer spectroscopy as a function of temperature

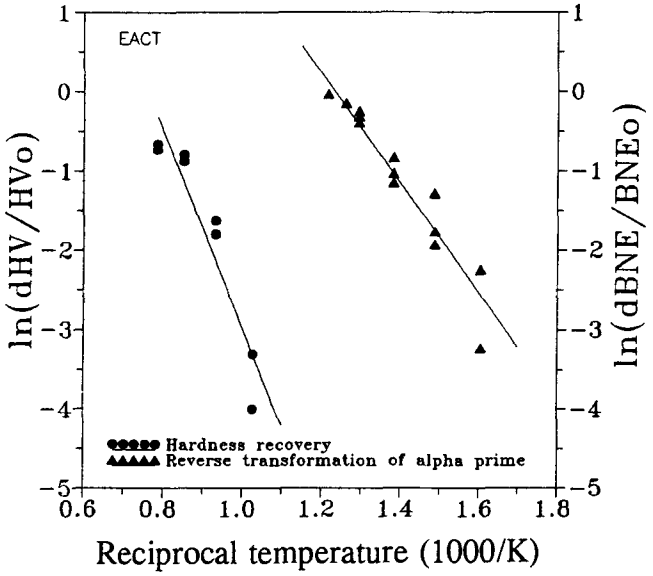

Fig. 6 Arrhenius-type plot of BN energy and hardness results

along the shear bands within the austenite grains. The saturation polarization of the α′-phase calculated from the data of Fig. 3 was 265.5 mT.

4. Conclusions

Many applications require control of the amount of ε- and α′-martensites in cold-worked stainless steels, because these phases are detrimental to stress corrosion resistance and hydrogen embrittlement. In the present work, the microstructure of the stainless steel specimens was characterized by magnetic Barkhausen measurement, magnetic saturation polarization, hardness measurement, scanning electron microscopy, and Mössbauer spectroscopy. The BN energy measurement was calibrated by using the results of conversion electron Mössbauer spectroscopy.

The suggested method of BN measurement was found to be a useful nondestructive and quantitative way to measure the amount of α′-martensite phase in austenitic stainless steels. The BN energy measurement was calibrated using the conversion electron Mössbauer spectroscopic technique.

In conclusion:

- The Barkhausen noise energy was found to be linearly proportional to the amount of α′-martensite.
- It was proved that α′-martensite forms continuously during cold work. Even the slightest deformation produced α′-phase, and the amount of α′-phase increased rapidly up to 50% strain.
- It was found that the appearance of α′-martensite during cold work contributes significantly to hardness. In cold-worked specimens above 600 °C, carbides precipitated within the grains, especially at the shear bands, played a role similar to α′-martensite in the hardening process. They prevented dislocation movement and kept hardness at the high level that corresponds to the cold-worked state.
- The activation energy of the reversion of α′-martensite to austenite was determined from BN energy results. The virtual activation energy of the hardness recovery process was also determined.
- The saturation polarization (J_{max}) and the coercive force (H_c) of the ferromagnetic α′-phase was determined.
- The suggested Barkhausen measuring method was found to be an effective tool for studying the transformation mechanisms of austenite to α′-martensite during deformation and the reverse process during heat treatment.

References

1. R.P. Reed, The Spontaneous Martensitic Transformation in 18 pct Cr, 8 pct Ni Steels, *Acta Metall.*, Vol 10, 1962, p 865-877
2. M.C. Mataya, M.J. Carr, and G. Krauss, The Bauschinger Effect in a Nitrogen-Strengthened Austenitic Stainless Steel, *Mater. Sci. Eng.*, Vol 57 (No. 2), 1983, p 205-222
3. P. Lacombe, B. Baroux, and G. Beranger, Ed., *Stainless Steels*, Les Editions de Physique Les Ulis, Les Ulis, France, 1993, p 551-569
4. P. Lacombe, B. Baroux, and G. Beranger, Ed., *Stainless Steels*, Les Editions de Physique Les Ulis, Les Ulis, France, 1993, p 74-79
5. D. Rousseau, G. Blanc, R. Tricot, and A. Gueussier, *Mém. Sci. Rev. Metall.*, Vol LXVII, 1970, p 315-333
6. J.R. Davis, Ed., *ASM Specialty Handbook: Stainless Steels*, ASM International, 1994, p 291, 445, 491
7. J. Ginsztler, I. Mészáros, L. Dévényi, B. Hidasi, and J.H. Potgieter, Magnetic Investigation of Stainless Steels, *Int. J. Pressure Vessels Piping*, Vol 61, 1995, p 471-478
8. I. Mészáros, L. Dévényi, B. Hidasi, J. Ginsztler, and K.A. Leich, Magnetic Testing of Structural Changes of Power Plant Steels, *Materials Performance, Maintenance and Plant Life Assessment*, I. Le May, P. Mayer, P.R. Roberge, and V.S. Sastry, Ed., Metallurgical Society of the Canadian Institute of Mining and Petroleum, 1994, p 145-151
9. A. Vértes, I. Czakó-Nagy, Mössbauer Spectroscopy and Its Applications to Corrosion Studies, *Electrochim. Acta*, Vol 34, 1989, p 721
10. V. Shrinivas, S.K. Varma, and L.E. Murr, Deformation-Induced Martensitic Characteristics in 304 and 316 Stainless Steels during Room-Temperature Rolling, *Metall. Mater. Trans. A*, Vol 26A, 1995, p 661-671
11. U. Dehlinger, *Theoretische Metallkunde*, Springer-Verlag, Berlin, 1955.